Haci Ozisik[a], Engin Deligoz[b], Kemal Colakoglu[c], Gokhan Surucu[c]
[a] BOTE Department, Aksaray University, Aksaray, Turkey
[b] Department of Physics, Aksaray University, Aksaray, Turkey
[c] Department of Physics, Gazi University, Ankara, Turkey

Ab-initio studies of some rare-earth borides: CeB_2, PrB_2, NdB_2, and PmB_2

https://doi.org/10.3139/146.110942

The structural, mechanical and thermal properties of CeB_2, PrB_2, NdB_2, and PmB_2 compounds in hexagonal AlB_2-type (P6/mmm) and ReB_2-type structures ($P6_3/mmc$) are investigated using density functional theory. The results indicate that those compounds with hexagonal AlB_2 structure are the most stable among the considered structures. The mechanical properties are calculated according to the elastic constants by means of the Voigt–Reuss–Hill averaging scheme. The temperature dependence of various quantities such bulk modulus, Debye temperature, thermal expansion, heat capacity, and Grüneisen parameter have been analyzed using the quasi-harmonic Debye model.

Keywords: Structural properties; Elastic properties; Thermodynamic properties; Rare-earth borides

1. Introduction

The physical properties of binary boride compounds have recently been attracting much interest due to the discovery of striking phenomena such as the high-temperature superconductivity in MgB_2 [1, 2]. They exhibit unique properties such as high melting points, high hardness values, and excellent oxidation resistance and also have interesting elastic, catalytic, and magnetic properties [3–10]. Hence, these compounds are promising materials for new heat-resistant, corrosion-resistant, and wear-resistant alloys and coatings [11]. The investigation of binary boride compounds is a growing area of material science in the search for new materials and properties due to their technological applications.

Rare-earth borides have a wide diversity of structural, physical, and physico-chemical properties and the presence of rare-earth metals in the boride lattice leads to a wide diversity of electrical and magnetic properties [12]. They possess good emissive properties and are used as cathode materials in emission electronics such as electron microscopes, Auger spectrometers, and microanalyzers [13]

RB_2 (R = Ce, Pr, Nd, Pm) compounds belong to the family of rare-earth borides and their physical properties are not sufficiently known so far. Zazoua et al. [14] have investigated mechanical properties and magnetic phase stability of these compounds. The electronic structure and magnetic behavior of hexagonal RB_2 have been studied using ab-initio density functional theory [15]. Recently, we [16] have presented the lattice dynamical properties for these compounds. These studies [14–17] suggest that rare-earth diborides in AlB_2 structure might be a potential candidate for hard materials.

The aim of this paper is to perform a theoretical investigation of structural, elastic and thermal properties of CeB_2, PrB_2, NdB_2, and PmB_2 compounds with the hexagonal AlB_2-type structure (P6/mmm) and ReB_2-type structure using first-principles calculations. In this study, the elastic properties in hexagonal ReB_2-type structure and thermal properties in hexagonal AlB_2 and ReB_2-type structures have investigated for the first time.

2. Methods and calculations

The calculations have been carried out using the Vienna ab-initio simulation package (VASP) code [18–21]. We have used the generalized gradient approximation (GGA) for the description of the exchange-correlation energy with both PBE [22] and PBESol [23] prescriptions. The electron–ion interaction was considered in the form of the projector-augmented-wave (PAW) method with plane wave up to energy of 750 eV. For k-space summation, the $11 \times 11 \times 11$ and $8 \times 8 \times 8$ Monkhorst and Pack [24] gamma centered grids of k-points have been used for AlB_2 and ReB_2 in structures, respectively. The energy difference for various k-meshes above this values does not change the total energy by more than 1 meV. The standard PAW pseudo-potential of B element was used. For Ce–Pm elements, f-electrons were partly kept frozen in the core, which is the standard model for the treatment of localized f-electrons. Hence, the trivalent pseudo-potential was used for these elements.

In order to obtain the thermodynamic properties of RB_2 (R = Ce, Pr, Nd, Pm) compounds, we use the well known quasi-harmonic Debye model [25–30]. The quasi-harmonic Debye model [25] in which the non-equilibrium Gibbs function $G^*(V; P, T)$ takes the form of

$$G^*(V;P,T) = E(V) + PV + A_{\mathrm{vib}}[\theta(V);T] \qquad (1)$$

is introduced. In Eq. (1), $E(V)$ is the total energy for per unit cell of these compounds, PV corresponds to the constant hydrostatic pressure condition, $\theta(V)$ is the Debye temperature and A_{vib} is the vibrational Helmholtz free energy and can be written as [26–29]

$$A_{\mathrm{vib}}(\theta,T) = nkT\left[\frac{9\theta}{8T} + 3\ln\left(1 - e^{-\frac{\theta}{T}}\right) - D\left(\frac{\theta}{T}\right)\right] \qquad (2)$$

© 2013 Carl Hanser Verlag, Munich, Germany www.ijmr.de Not for use in internet or intranet sites. Not for electronic distribution.

where n is the number of atoms per formula unit, $D\left(\frac{\theta}{T}\right)$ is the Debye integral. For an isotropic solid, θ is expressed as [28]

$$\theta_D = \frac{\hbar}{k}\left[6\pi V^{1/2} n\right]^{1/3} f(\sigma)\sqrt{\frac{B_s}{M}} \tag{3}$$

where M is the molecular mass per unit cell and B_s is the adiabatic bulk modulus, which is given approximately by the static compressibility

$$B_s \approx B(V) = V\frac{d^2E(V)}{dV^2} \tag{4}$$

Therefore, the non-equilibrium Gibbs function $G^*(V; P, T)$ as a function of $(V; P, T)$ can be minimized with respect to volume V as:

$$\left[\frac{\partial G^*(V;P,T)}{\partial V}\right]_{P,T} = 0 \tag{5}$$

By solving Eq. (5), one can obtain the thermal equation-of-state (eos) $V(P, T)$. The heat capacity at constant volume C_v and the thermal expansion coefficient (α) are given [30] as follows:

$$C_v = 3nk\left[4D\left(\frac{\theta}{T}\right) - \frac{3\theta/T}{e^{\theta/T}-1}\right] \tag{6}$$

$$\alpha = \frac{\gamma C_v}{B_T V} \tag{7}$$

Here γ represents the Grüneisen parameter and its general expression is given as

$$\gamma = -\frac{d\ln\theta(V)}{d\ln V} \tag{8}$$

3. Results and discussion

3.1. Structural and mechanical properties

Wyckoff positions and calculated atomic positions for the considered structures are given in Table 1. The total energy was minimized by relaxing the structural parameters using a conjugate gradient optimization method. The obtained lattice parameters, bond distances are listed in Table 2 together with previous theoretical values. The results of PBESol calculations are lower (about 2 %) than PBE calculations. Compared with the LDA and LSDA + U calculations of Zazoua et al. [14], the calculated lattice parameters for considered compounds with AlB_2 structure are higher (about 6–8 %) than the other theoretical results [14]. We note that the anion atoms are the same in these compounds, the cation sizes are different. A typical feature of the rare earth series is that the lattice parameters and bond distance decrease with atomic number, which can be interpreted as gradual localization of f-electrons in the series. The calculated total energies indicate that hexagonal structures within AlB_2 structure are energetically more favorable than those of ReB_2 structure. CeB_2 possesses the largest bond strength among these compounds. To investigate the possibility of experimentally synthesizing RB_2 compounds we have studied the formation energy. The calculated formation energies are also given in Table 2. The calculated negative formation energies have indicated that all structures are thermodynamically stable. From Table 2, it can be seen that PbB_2 with AlB_2 structure possesses the lowest formation energy among the considered RB_2 compounds.

In order to study the mechanical properties, we have calculated the elastic constants using the "stress–strain" relations [31], and the findings are listed in Table 3. The Born mechanical stability criterion for hexagonal structure is given below [32]:

$$C_{11} > 0, C_{11} - C_{12} > 0, C_{44} > 0, \text{and}$$
$$(C_{11} + C_{12})C_{33} - 2C_{12}^2 > 0 \tag{9}$$

Our calculated elastic constants satisfy the Born stability criteria, suggesting that AlB_2 and ReB_2 structures are mechanically stable. Our results of PBESol calculations are higher (about 2 %) than the PBE calculation. The calculated elastic constants for AlB_2 structure are lower/higher than the other theoretical results [14]. We attribute this discrepancy to the difference in the lattice parameters used in our calculations and given in Ref. [14]. It is, also, widely known that the main reason for a discrepancy in the calculated lattice parameters, on the fundamental level, may arise from different calculation techniques, pseudopotential or exchange-correlation functional used in calculations.

The present C_{33} is higher than the C_{11} for all compounds. Thus, the a-axis is more compressible than the c-axis. It is known that the elastic constants C_{44} and C_{66} are the most important parameters indirectly governing the indentation hardness of a material. The large C_{44} means strong ability to resist monoclinic shear distortion in the (100) plane, and the C_{66} relates to the resistance to shear in the <110> direction. The calculated C_{44} (143.8 GPa) and C_{66} (116.7 GPa) for PmB_2 with AlB_2 structure is higher than the other compounds.

Table 1. Atomic positions and space group of probable phase AB_2 type compounds.

Structure	Braves	Space Group (Number)	Strukturb. Designation	Atom	Site	Internal Parameters
AlB_2-Type	Hexagonal	P6/mmm (191)	C32	R B	1a (0, 0, 0) 2d (1/3, 2/3, 1/2)	
ReB_2-Type	Hexagonal	$P6_3/mmc$ (194)		R B	2c (1/3, 2/3, 1/4) 4f (1/3, 2/3, z)	$z = 0.6385$

© 2013 Carl Hanser Verlag, Munich, Germany www.ijmr.de Not for use in internet or intranet sites. Not for electronic distribution.

Table 2. The calculated equilibrium lattice parameters (a, and c in Å), the R–R, R–B bond distance (in Å), and the formation energies (ΔH_f in eV/f.u.) for RB_2 (R = Ce, Pr, Nd, Pm) in AlB_2 and ReB_2 structures.

Structure	R	a	c	d_{R-R}	d_{R-B}	d_{B-B}	ΔH_f	Ref.
AlB_2-Type	Ce	3.362	4.253	3.362	2.879	1.941	–5.12827	Present (PBE)
		3.332	4.212	3.332	2.852	1.924	–5.38584	Present (PBESol)
		3.152	4.113					LSDA[a]
		3.180	4.112					LSDA + U[a]
	Pr	3.348	4.19	3.348	2.851	1.933	–5.32763	Present (PBE)
		3.317	4.149	3.317	2.824	1.915	–5.58849	Present (PBESol)
		3.092	4.080					LSDA[a]
		3.160	3.969					LSDA + U[a]
	Nd	3.338	4.135	3.338	2.826	1.927	–5.49377	Present (PBE)
		3.307	4.094	3.307	2.799	1.909	–5.75696	Present (PBESol)
		3.108	4.093					LSDA[a]
		3.202	4.039					LSDA + U[a]
	Pm	3.33	4.077	3.320	2.802	1.923	–5.66101	Present (PBE)
		3.299	4.037	3.299	2.775	1.904	–5.93221	Present (PBESol)
		3.142	4.089					LSDA[a]
		3.195	4.069					LSDA + U[a]
ReB_2-Type	Ce	4.702	6.913	4.395	2.682	1.548	–2.69923	Present (PBE)
		4.622	6.842	4.339	2.643	1.557	–2.56449	Present (PBESol)
	Pr	4.644	6.862	4.354	2.656	1.549	–2.77472	Present (PBE)
		4.57	6.768	4.291	2.605	1.559	–2.65359	Present (PBESol)
	Nd	4.593	6.822	4.321	2.636	1.550	–2.83411	Present (PBE)
		4.519	6.729	4.258	2.585	1.56	–2.72505	Present (PBESol)
	Pm	4.543	6.786	4.289	2.617	1.551	–2.90316	Present (PBE)
		4.543	6.786	4.289	2.617	1.551	–2.79279	Present (PBESol)

[a] LSDA and LSDA + U values taken from Ref. [14].

Table 3. The calculated elastic constants (in GPa) for RB_2 (R = Ce, Pr, Nd, Pm) with AlB_2 and ReB_2 structures.

Structures	R	C_{11}	C_{12}	C_{13}	C_{33}	C_{44}	C_{66}	Refs.
AlB_2-Type	Ce	233.5	61.2	79	264.5	128.8	86.2	Present (PBE)
		245.9	70.3	84.7	282.3	136.8	87.8	Present (PBESol)
		286.86	113.94	108.75	400.80	231.83	86.46	LSDA[a]
		281.32	86.57	116.78	371.51	217.09	97.38	LSDA + U[a]
	Pr	249.5	53.4	79.2	273.2	134.4	98.1	Present (PBE)
		261.7	63.4	84.7	291	143.4	99.1	Present (PBESol)
		249.77	91.64	81.75	349.09	194.70	79.06	LSDA[a]
		295.73	105.97	111.68	381.24	186.73	94.88	LSDA + U[a]
	Nd	263	46.4	79.7	281.5	138.9	108.3	Present (PBE)
		276	56	85	297	148.2	110	Present (PBESol)
		261.77	105.76	90.76	352.24	241.56	78.00	LSDA[a]
		295.38	70.88	97.519	313.268	166.037	112.25	LSDA + U[a]
	Pm	273.1	39.6	79.8	291.7	143.8	116.7	Present (PBE)
		287.2	49.3	84.9	304.1	153	119	Present (PBESol)
		256.84	104.04	81.47	306.80	208.46	76.40	LSDA[a]
		317.77	43.02	92.45	269.41	159.16	137.37	LSDA + U
ReB_2-Type	Ce	89.9	34.3	19.6	252.4	12.4	27.8	Present (PBE)
		99.3	35.6	25.9	251.6	13.2	31.8	Present (PBESol)
	Pr	93.9	35	20.8	258.6	12.9	29.4	Present (PBE)
		104.8	37.1	21.5	273.7	13.3	33.8	Present (PBESol)
	Nd	97.7	35.9	21.3	264.7	13.3	30.9	Present (PBE)
		109	38	22.6	280	13.9	35.5	Present (PBESol)
	Pm	101.7	37.1	21.3	272.8	13.8	32.3	Present (PBE)
		101.7	37.1	21.3	272.7	13.8	32.3	Present (PBESol)

[a] LSDA and LSDA + U values taken from Ref. [14].

© 2013 Carl Hanser Verlag, Munich, Germany www.ijmr.de Not for use in internet or intranet sites. Not for electronic distribution.

The presented bulk modulus (B) and shear modulus (G) were derived from from the Voigt–Reuss–Hill (VRH) approximation [33]. The Voigt–Reuss–Hill approximation is an average of the two bounds, namely the lower bound of Voigt and upper bound of Reuss. The Young's modulus (E) and Poisson's ratio (v) are obtained by the following formulas:

$$E = 9BG/(3B + G); v = (3B - 2G)/2(3B + G) \qquad (10)$$

The calculated bulk modulus, shear modulus, Young's modulus, and Poisson's ratio are given in Table 4 together with other theoretical values [14]. The values of the bulk moduli indicate that PmB_2 in the AlB_2 is the least compressible material. The shear modulus, a measurement of resistance to shape change, is more pertinent to hardness and the larger shear modulus is mainly due to its larger C_{44}. The calculated shear modulus for AlB_2-type structure is higher than for ReB_2 structure, and PmB_2 with AlB_2 structure possesses the largest shear modulus among the other compounds.

If the value of E is large, the material is stiff. In this context, due to the higher value of Young's modulus (281.6 GPa) for PmB_2 with AlB_2 structure it is relatively stiffer than the other compounds. If the value of E, which has an impact on the ductility increases, the covalent nature of the material also increases. From Table 4, one can see that E increases when as we move from Ce to Pm for the considered structures.

Poisson's ratio provides more information about the characteristic of the bonding forces than any of the other elastic constants. 0.25 and 0.5 are the lower and upper limits for central force solids, respectively [34]. Our v values for ReB_2 structure are close to the value of 0.3 indicating the inter-atomic forces are predominantly central forces. The obtained values are less than 0.25 for AlB_2 structure, which indicates that the interatomic forces are dominant.

According to the Pugh formulation [35], high B/G ratio is associated with ductility, whereas a low value corresponds to brittleness. The critical value that separates brittle and ductile materials is around 1.75. If $B/G > 1.75$, the material behaves in a ductile manner; otherwise the material behaves in a brittle manner. The B/G ratios of AlB_2 structure are less than 1.75. Hence, the compounds with AlB_2 structure are classified as brittle in nature. Moreover, for covalent and ionic materials the typical relations between bulk and shear modulus are $G \cong 1.1B$ and $G \cong 0.8B$, respectively [36]. The present value of $G/B \cong 0.77$ strongly supports the ionic contribution to inter atomic bonding for AlB_2-type structure.

As is well known, the hardness is related to the elastic and plastic properties of a material. The microhardness is calculated in terms of the computed data using the following relations [37]:

$$H_{\text{Chen}} = 2(k^2G)^{0.585} - 3 \qquad (11)$$

Table 4. The calculated bulk modulus (B, in GPa), isotropic shear modulus (G, in GPa), Young's modulus (E, in GPa), Poisson's ratio (v), hardness (H_{Chen}, in GPa), Debye temperature (θ_D, in K) for RB_2 (R = Ce, Pr, Nd, Pm) with AlB_2 and ReB_2 structures.

Structures	R	B	G	E	N	B/G	H_{Chen}	θ_D	Refs.
AlB_2-Type	Ce	129.4	100.8	240.0	0.19	1.283	19.2	540.1	Present (PBE)
		138.7	105.4	252.2	0.2	0.76	19.1	550.1	Present (PBESol)
		169.68	152.90				18.771		LSDA[a]
		174.93	147.25				17.428		LSDA + U[a]
	Pr	132.3	109	256.5	0.18	1.213	21.8	547.3	Present (PBE)
		141.7	113.8	269.3	0.18	0.8	21.7	556.9	Present (PBESol)
		150.99	133.26				19.540		LSDA[a]
		181.26	136.56				18.666		LSDA + U[a]
	Nd	134.8	115.7	269.8	0.17	1.165	23.9	565.9	Present (PBE)
		144	120.9	283.3	0.17	0.84	23.9	576.1	Present (PBESol)
		161.15	151.46				19.091		LSDA[a]
		159.54	131.40				17.379		LSDA + U[a]
	Pm	136.6	121.8	281.6	0.16	1.121	26.0	573.7	Present (PBE)
		145.7	127.1	295.4	0.16	0.87	26.0	583.5	Present (PBESol)
		150.49	135.56				18.359		LSDA[a]
		151.20	136.27				17.357		LSDA + U[a]
ReB_2-Type	Ce	59.9	27.3	71	0.30	2.194	2.5	307.6	Present (PBE)
		65.1	28.9	75.5	0.31	0.44	2.5	314.3	Present (PBESol)
	Pr	62.1	28.4	73.9	0.30	2.186	2.7	305.7	Present (PBE)
		67.1	30.7	79.9	0.3	0.46	2.9	315.4	Present (PBESol)
	Nd	64	29.4	76.4	0.30	2.176	2.8	312.1	Present (PBE)
		69.4	31.9	82.9	0.3	0.46	3.1	322.5	Present (PBESol)
	Pm	66.1	30.6	79.5	0.30	2.16	3.0	314.3	Present (PBE)
		66.1	30.6	79.5	0.3	0.46	3.0	314.3	Present (PBESol)

[a] LSDA and LSDA + U values taken from Ref. [14].

© 2013 Carl Hanser Verlag, Munich, Germany www.ijmr.de Not for use in internet or intranet sites. Not for electronic distribution.

© 2013 Carl Hanser Verlag, Munich, Germany www.ijmr.de Not for use in internet or intranet sites. Not for electronic distribution.

where k is Pugh's modulus ratio ($k = G/B$), G is the shear modulus. The obtained results are given in Table 4. Our results indicate that the CeB_2, PrB_2, NdB_2, and PmB_2 compounds with hexagonal AlB_2-type structure are hard materials and the hardness of PmB_2 is higher than the others. The high hardness of PmB_2 can be attributed to the strong covalent-ionic Pb–B bonds. Our calculated Debye temperature is also given in Table 4, following the procedure detailed in Ref. [38–40]. The PmB_2 compound with AlB_2 structure possesses the largest Debye temperature among the other compounds. For an isotropic crystal, the values of A_1, A_2 and A_3 are equal to 1, while any value smaller or greater than 1 is a measure of the degree of shear anisotropy possessed by the crystal. From Table 5, it can be seen that CeB_2 with AlB_2 structure exhibits low anisotropy for A_1.

Table 5. The calculated shear anisotropic factors (A_1 and A_3) for different planes.

Materials	Structure	A_1	A_3	Refs.
CeB_2	AlB_2	1.52	1.00	Present (PBE)
		1.52	1.00	Present (PBESol)
	ReB_2	0.16	1.00	Present (PBE)
		0.18	1.00	Present (PBESol)
PrB_2	AlB_2	1.48	1.00	Present (PBE)
		1.5	1.00	Present (PBESol)
	ReB_2	0.17	1.00	Present (PBE)
		0.16	1.00	Present (PBESol)
NdB_2	AlB_2	1.44	1.00	Present (PBE)
		1.47	1.00	Present (PBESol)
	ReB_2	0.17	1.00	Present (PBE)
		0.16	1.00	Present (PBESol)
PmB_2	AlB_2	1.42	1.00	Present (PBE)
		1.45	1.00	Present (PBESol)
	ReB_2	0.17	1.00	Present (PBE)
		0.17	1.00	Present (PBESol)

3.2. Thermal properties

The thermal properties are determined in the temperature range from 0 to 1 000 K in GGA-PBE approximation for considered compounds, where the quasi-harmonic model remains fully valid.

The variations in the bulk modulus with temperature at zero pressures are shown in Fig. 1. It can be seen from Fig. 1 that bulk modulus decreases with the temperature at the same pressure. When $T < 100$ K, the bulk modulus is nearly constant, but it drops remarkably when $T > 100$ K.

The heat capacity at constant volume C_v at different temperatures T is shown in Fig. 2. It can be seen that C_v increases slowly with temperature and it almost approaches a constant called the Dulong–Petit limit at higher temperatures. When $T < 400$ K, the heat capacity is strongly dependent on the temperature. This is due to the anharmonic approximations of the Debye model [30].

The variations in the thermal expansion coefficient (α) with temperature are shown in Fig. 3. The thermal expansion coefficient increases with T^3 at lower temperatures (about $T < 200$ K) and gradually approaches a linear increase at high temperatures and then the increasing trend

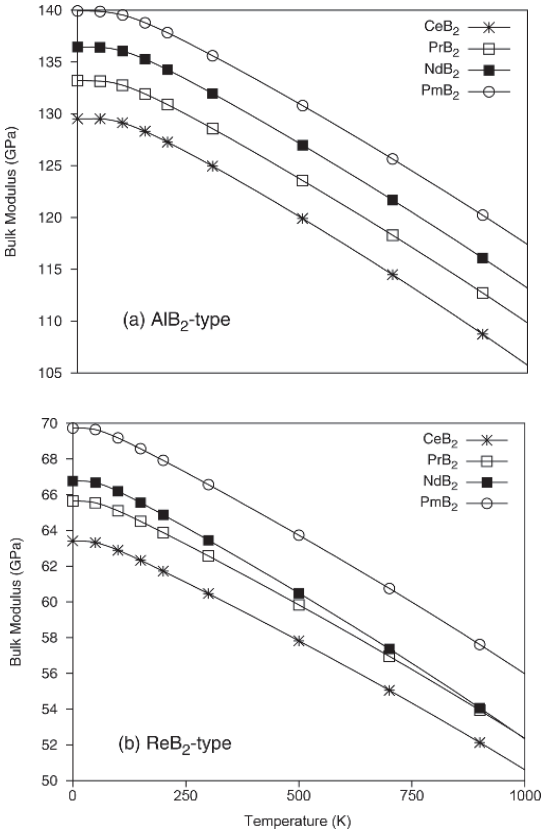


Fig. 1. Variation in the bulk modulus with temperature at zero pressure.

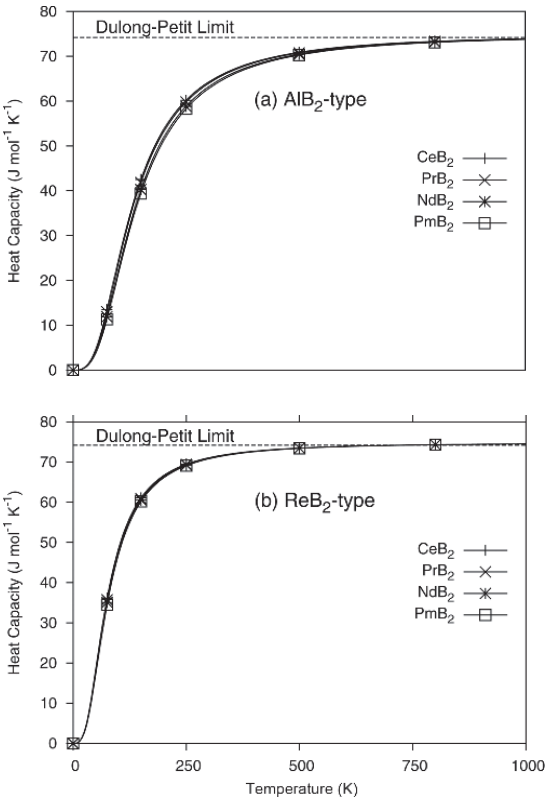


Fig. 2. Variation in the heat capacity with temperature at zero pressure.

becomes gentler. It is noteworthy that the high temperature dependence of the thermal expansion coefficient is not linear; this is an indication of the inadequacy of the quasi-harmonic approximation at high temperatures [41]. The calculated thermal expansion coefficients with ReB_2 structure (about $4.6-5.0\times10^{-5}$ K^{-1}) are higher than that with AlB_2 structure (about $3.4-3.7\times10^{-5}$ K^{-1}) at 300 K.

In Fig. 4, we show variation in the Debye temperature as a function of temperature. The temperature effects on heat capacity (C_v) and Debye temperature are similar. The calculated Debye temperatures with ReB_2 structure (about 306 – 317 K) are lower than that with AlB_2 structure (about 532 – 573 K) at 300 K and PmB_2 with AlB_2 has the highest values. The Debye temperature at the temperature of 1 000 K is lower than that 300 K, which shows the fact that the vibration frequency of the particles in these compounds changes with temperature [42].

Grüneisen parameter, which describes the alteration in a crystal lattice's vibration frequency, can reasonably predict the anharmonic properties of a solid, such as the temperature dependence of phonon frequencies and lattice volume [43]. The calculated relationship of the Grüneisen parameter with temperature is plotted in Fig. 5. As the Grüneisen parameter has anharmonic behavior, we would not expect linear variation with temperature.

4. Conclusion

The structural, elastic and mechanical properties of CeB_2, PrB_2, NdB_2, and PmB_2 compounds were predicted by

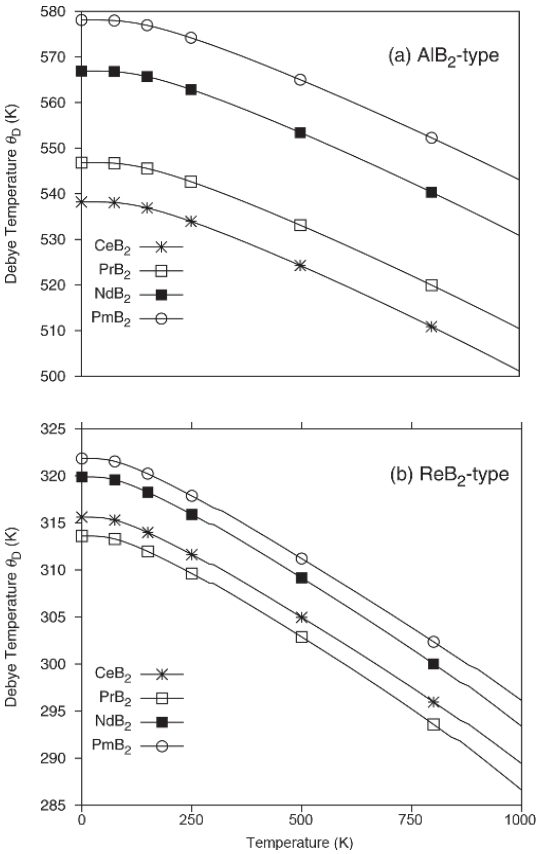


Fig. 4. Variation in the Debye temperature with temperature at zero pressure.

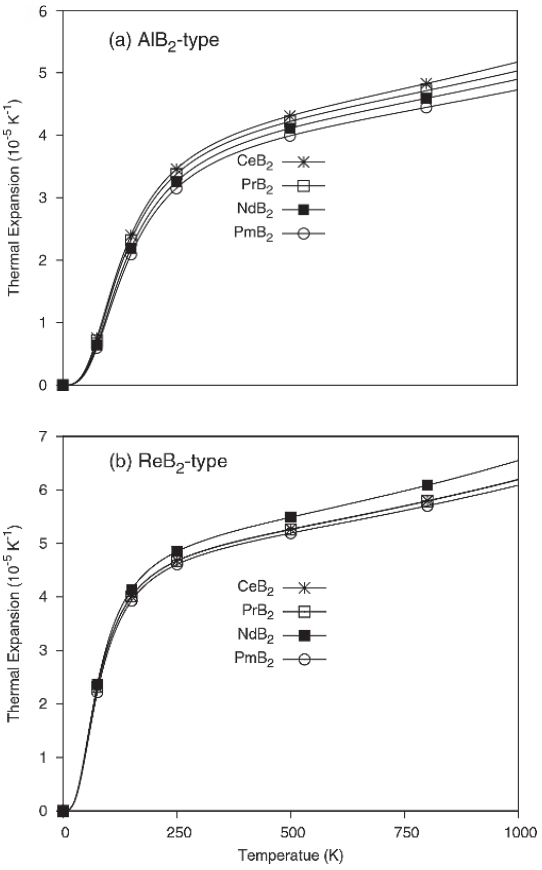


Fig. 3. Variation in the thermal expansion coefficient with temperature at zero pressure.

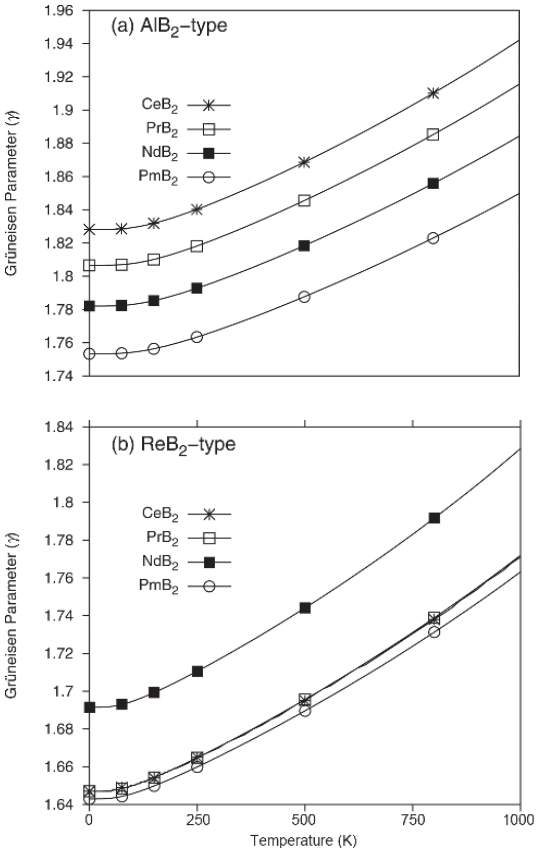


Fig. 5. Variation in the Grüneisen parameter with temperature at zero pressure.

© 2013 Carl Hanser Verlag, Munich, Germany www.ijmr.de Not for use in internet or intranet sites. Not for electronic distribution.

means of first-principles calculations. The thermal properties have also been obtained successfully using the quasi-harmonic Debye model. Our results suggest that the AlB_2 structure for all compounds is the most stable structure, and all rare-earth compounds are mechanically stable with both AlB_2 and ReB_2 structures. The CeB_2, PrB_2, NdB_2, and PmB_2 compounds with hexagonal AlB_2-type structure are also hard materials. The variation in bulk modulus, Debye temperature, thermal expansion, heat capacity, and the Grüneisen parameter with temperature were analyzed systematically in the range from 0 to 1 000 K.

References

[1] J. Nagamatsu, N. Nakagawa, T. Muranaka, Y. Zenitani, J. Akimitsu: Nature 410 (2001) 63. PMid:11242039; DOI:10.1038/35065039
[2] T. Mori, F. Zhang, T. Tanaka: J. Phys. Condens. Mater. 13 (2001) L423. DOI:10.1088/0953-8984/13/20/105
[3] R.B. Kaner, J.J. Gilman, S.H. Tolbert: Science 308 (2005) 1268. PMid:15919983; DOI:10.1126/science.1109830
[4] W. Zhou, H. Wu, and T. Yildirim: Phys. Rev. B 76 (2007) 184113. DOI:10.1103/PhysRevB.76.024433
[5] H.Y. Chung, M.B. Weinberger, J.B. Levine, A. Kavner, J.M. Yang, S.H. Tolbert, R.B. Kaner: Science 316 (2007) 436. PMid:17446399; DOI:10.1126/science.1139322
[6] H.Y. Chung, M.B. Weinberger, J. Yang, S.H. Tolbert, R.B. Kaner: Appl. Phys. Lett. 92 (2008) 261904. DOI:10.1063/1.2826271
[7] R.W. Cumberland, M.B. Weinberger, J.J. Gilman, S.M. Clark, S.H. Tolbert, R.B. Kaner: J. Am. Chem. Soc. 127 (2005) 7264. PMid:15898746; DOI:10.1021/ja043806y
[8] M.I. Matkovich, G.V. Samsonov, P. Hagenmuller, T. Lundstrom, in: M.I. Matkovich (Eds.), Boron and Refractory Borides, Springer-Verlag, Berlin (1977). DOI:10.1007/978-3-642-66620-9
[9] G.V. Samsonov, I.M. Vinitskii: Handbook of Refractory Compounds Metallurgiya, Moscow (1976).
[10] T.I. Serebryakova, V.A. Neronov, P.D. Peshev: High-Temperature Borides Metallurgiya, Moscow (1991).
[11] I.R. Shein, A.L. Ivanovskii: Phys. Rev. B 73 (2006) 144108. DOI:10.1103/PhysRevB.73.144108
[12] V.V. Novikov, A.V. Matovnikov: Inorganic Materials 44 (2008) 134. DOI:10.1134/S002016850802009X
[13] A.V. Matovnikov, V.S. Urbanovich, T.A. Chukina, A.A. Sidorov, V.V Novikov: Inorganic Materials 45 (2009) 366. DOI:10.1134/S0020168509040062
[14] F. Zazoua, S. Kacimi, M. Djermouni, A. Zaoui: J. Appl. Phys. 110 (2011) 014908. DOI:10.1063/1.3607268
[15] S. Kacimi, B. Bekkouche, A. Boukortt, F. Zazoua, M. Djermouni, A. Zaoui: Phys. Status Solidi B 249 (2012) 1470. DOI:10.1002/pssb.201147542
[16] H. Ozisik, K. Colakoglu, E. Deligoz, E. Ateser: Comp. Mater. Sci. 68 (2013) 307. DOI:10.1016/j.commatsci.2012.11.003
[17] E. Deligoz, H. Ozisik, K. Colakoglu, G. Surucu, Y.O. Ciftci: J. Alloy. Compd. 509 (2010) 1711. DOI:10.1016/j.jallcom.2010.10.015
[18] G. Kresse, J. Furthmuller: Comp. Mater. Sci. 6 (1996) 15. DOI:10.1016/0927-0256(96)00008-0
[19] G. Kresse, D. Joubert: Phys. Rev. B 59 (1999) 1758. DOI:10.1103/PhysRevB.59.1758
[20] G. Kresse, J. Furthmuller: Phys. Rev. B 54 (1996) 11169. DOI:10.1103/PhysRevB.54.11169
[21] P.E. Blochl: Phys. Rev. B 50 (1994) 17953. DOI:10.1103/PhysRevB.50.17953
[22] J.P. Perdew, K. Burke, M. Ernzerhof: Phys. Rev. Lett. 77 (1996) 3865. PMid:10062328; DOI:10.1103/PhysRevLett.77.3865
[23] J.P. Perdew, A. Ruzsinszky, G.I. Csonka, O.A. Vydrov, G.E. Scuseria, L.A. Constantin, X. Zhou, K. Burke: Phys. Rev. Lett. 100 (2008) 136406. PMid:18517979; DOI:10.1103/PhysRevLett.100.136406
[24] H.J. Monkhorst, J.D. Pack: Phys. Rev. B 13 (1976) 5188. DOI:10.1103/PhysRevB.13.5188
[25] A.A. Maradudin, E.W. Montroll, G.H. Weiss, I.P. Ipatova: Theory of Lattice Dynamics in the Harmonic Approximation, Academic Press (1971).
[26] M.A. Blanco: PhD Thesis, Universidad de Oviedo, Spain (1997).
[27] M.A. Blanco, A.M. Pendás, E. Francisco, J.M. Recio, R. Franco: J. Mol. Struct. Theochem 368 (1996) 245. DOI:10.1016/S0166-1280(96)90571-0
[28] E. Francisco, J.M. Recio, M.A. Blanco, A.M. Pendás, A. Costales: J. Phys. Chem. A 102 (1998) 1595. DOI:10.1021/jp972516j
[29] E. Francisco, G. Sanjurjo, M.A. Blanco: Phys. Rev. B 63 (2001) 094107. DOI:10.1103/PhysRevB.63.094107
[30] M. Flórez, J.M. Recio, E. Francisco, M.A. Blanco, A.M. Pendás: Phys. Rev. B 66 (2002) 144112. DOI:10.1103/PhysRevB.66.144112
[31] Y.L. Page, P. Saxe: Phys. Rev. B 65 (2002) 104104. DOI:10.1103/PhysRevB.65.104104
[32] Z. Wu, E. Zhao, H. Xiang, X. Hao, X. Liu, J. Meng: Phys. Rev. B 76 (2007) 054115. DOI:10.1103/PhysRevB.75.054115
[33] R. Hill: Proceedings of the Physical Society. Section A 65 (1952) 349. DOI:10.1088/0370-1298/65/5/307
[34] H. Fu, D. Li, F. Peng, T. Gao, X. Cheng: Comp. Mater. Sci. 44 (2008) 774. DOI:10.1016/j.commatsci.2008.05.026
[35] S.F. Pugh: Phil. Mag. Series 7 45 (1954) 823.
[36] I.R. Shein, A.L. Ivanovskii: J. Phys. Condens. Mat. 20 (2008) 415218. DOI:10.1088/0953-8984/20/41/415218
[37] X.Q. Chen, H. Niu, D. Li, Y. Li: Intermetallics 19 (2011) 1275. DOI:10.1016/j.intermet.2010.08.010
[38] I. Johnston, G. Keeler, R. Rollins, S. Spicklemire: Solid State Physics Simulations, The Consortium for Upper-Level Physics Software, Jhon Wiley, New York (1996).
[39] O.L. Anderson: J. Phys. Chem. Solids 24 (1963) 909. DOI:10.1016/0022-3697(63)90067-2
[40] E. Schreiber, O.L. Anderson, N. Soga: Elastic Constants and their Measurements, McGraw-Hill, New York (1973).
[41] F. Peng, H. Fu, X. Yang: Physica B 403 (2008) 2851. DOI:10.1016/j.physb.2007.12.016
[42] F. Peng, Q. Liu, H. Fu, X. Yang: Solid State Communi. 149 (2009) 56. DOI:10.1016/j.ssc.2008.10.010
[43] B. Yu, D. Chen, Q. Tang, C. Wang, D. Shi: J. Phys. Chem. Solids 71 (2010) 758. DOI:10.1016/j.jpcs.2009.11.011

(Received September 6, 2012; accepted March 20, 2013; online since April 30, 2013)

Bibliography

DOI 10.3139/146.110942
Int. J. Mater. Res. (formerly Z. Metallkd.)
104 (2013) 9; page 858 – 864
© Carl Hanser Verlag GmbH & Co. KG
ISSN 1862-5282

Correspondence address

Assoc. Prof. Dr. Engin Deligoz
Aksaray University
Department of Physics
Main Campus 68100
Aksaray
Turkey
Tel.: +90 382 2882160
Fax: +90 382 2882125
E-mail: edeligoz@yahoo.com

You will find the article and additional material by entering the document number **MK110942** on our website at *www.ijmr.de*

https://doi.org/10.3139/146.110942

© 2013 Carl Hanser Verlag, Munich, Germany www.ijmr.de Not for use in internet or intranet sites. Not for electronic distribution.